NANO LETTERS

pubs.acs.org/NanoLett

Particle Size Dependence of the Ionic Diffusivity

Rahul Malik,[†] Damian Burch,[†] Martin Bazant,[†,§] and Gerbrand Ceder*[,†]

[†]Department of Materials Science and Engineering, [†]Department of Mathematics, and [§]Department of Chemical Engineering, Massachusetts Institute of Technology, Cambridge, Massachusetts 02139

ABSTRACT Diffusion constants are typically considered to be independent of particle size with the benefit of nanosizing materials arising solely from shortened transport paths. We show that for materials with one-dimensional atomic migration channels, the diffusion constant depends on particle size with diffusion in bulk being much slower than in nanoparticles. This model accounts for conflicting data on $LiFePO_4$, an important material for rechargeable lithium batteries, specifically explaining why it functions exclusively on the nanoscale.

KEYWORDS Batteries, diffusion, nano, ab initio

The benefit of nanosizing materials on bulk transport is conventionally attributed to the higher surface-to-volume ratio and reduced transport length in nanoparticles.[1] The diffusion constants that govern mass transport are not often regarded as size-dependent, and macroscopic theories such as Fick's Law are implicitly assumed to be size-independent. We show that for materials with a one-dimensional (1D) diffusion mechanism, nanosizing is particularly advantageous for ionic transport, as the intrinsic diffusion constant is scale dependent and significantly reduced at large particle size. The material we focus on is $LiFePO_4$,[2] a well-known cathode material for rechargeable Li^+ ion batteries that only operates in batteries when in nanoform, though the results should be applicable to all materials with 1D diffusion. We show that the presence of point defects in one-dimensional transport paths makes the diffusion constant particle size-dependent, and that very high diffusivity at the nanoscale cannot be sustained in large crystals. In addition, we reconcile the observation of almost isotropic diffusion in large crystals with the strong anisotropic nature of Li mobility at the microscopic level.

Computational[3,4] and experimental[5] studies of $LiFePO_4$ indicate that Li^+ ion migration occurs preferentially via one-dimensional channels oriented along the [010] direction of the orthorhombic crystal structure. These channels are shown in Figure 1. In fact, Li^+ ion diffusion along a perfect b direction is calculated to be so rapid ($D \sim 10^{-8}$ cm^2 s^{-1}) that nanosize particles (100 nm) would be delithiated in much less than a second (0.01 s), and micrometer-size particles (1 μm) in a second if intrinsic Li^+ mobility in the material were rate-controlling.[4] These predictions are certainly commensurate with the high rate performance observed in nanosized $LiFePO_4$,[6−8] but studies of macroscopic $LiFePO_4$ exhibit much poorer and fundamentally different transport properties. Specifically, conductivity studies performed by Amin et al. on macroscopic (millimeter scale) $LiFePO_4$ single crystals[9] indicate that at ~150 °C the chemical diffusion coefficient of lithium is $\sim 10^{-9}-10^{-10}$ cm^2 s^{-1}, but diffusion coefficient measurements taken along the a, b, and c axes from the same study also indicate that the Li^+ ion diffusivity is significantly less anisotropic compared to computational calculations,[4] and experimental observations[5] of the Li^+ positions.

One-dimensional diffusion is significantly different than diffusion in 2D or 3D. For instance, one-dimensional diffusion will be impeded by the presence of immobile and low-mobility defects (shown as black circles in Figure 1b) residing in the diffusion path. In dimension 2 or higher, immobile point defects will not affect the rate of two-dimensional diffusion, as the diffusing species can simply move around the defect. Hence, the presence of point defects will have a drastic effect on the rate at which ions can move through the crystal. For any finite concentration of point defects in 1D diffusion channels, there will be some channel length above which channels contain on average two or more point

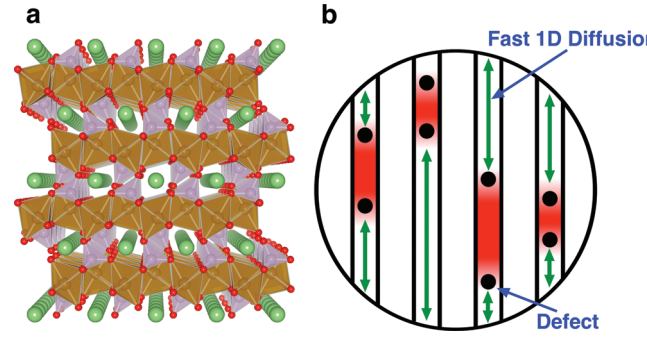

FIGURE 1. (a) Crystal structure of $LiFePO_4$ illustrating 1D Li^+ diffusion channels oriented along the [010] direction. (b) Schematic illustration of Li^+ diffusion impeded by immobile point defects in 1D channels.

* To whom correspondence should be addressed. E-mail: gceder@mit.edu.
Received for review: 07/6/2010
Published on Web: 08/26/2010

DOI: 10.1021/nl1023595 | *Nano Lett.* **2010,** *10,* 4123–4127

defects, thereby making sites inside the material inaccessible to Li^+ ions entering through either side of the tunnel opening (shown in red in Figure 1b). The channel-blocking concept allows us to illustrate the pathological nature of one-dimensional diffusion. If the diffusing ion cannot circumvent the defect, the macroscopic diffusion constant will become zero considering that $D \approx \langle r^2 \rangle / 2t$. If a channel is blocked, the mean-square displacement $\langle r^2 \rangle$ of an ion in the channel is capped, and at long times t the diffusivity goes to zero.

For one-dimensional diffusion to be sustainable in the macroscopic limit, it is required that the diffusing species can cross over between different 1D channels. While this is unlikely in perfect materials, defects such as vacancies in the atomic sites between the channels can make crossover possible. For $LiFePO_4$, we used ab initio density functional theory in the GGA+U approximation with previously defined parameters[10] to perform an exhaustive search of formation energies of possible point defects involving combinations of Li^+ vacancies and interstitials, Li^+ on Fe^{2+} sites, Fe^{2+} on Li^+ sites, Fe^{3+} on Fe^{2+}sites, and Fe^{2+} vacancies (hereafter referred to using Kroger−Vink notation as V_{Li}^{-}, $Li_i^{\bullet}$, Li_{Fe}^{-}, $Fe_{Li}^{\bullet}$, $Fe_{Fe}^{\bullet}$, and V_{Fe}^{2-}, respectively). The detailed results of this search will be reported elsewhere. We found that for all reasonable conditions of the external chemical potential of each species, the nearest neighbor antisite defect Li_{Fe}^{-}−$Fe_{Li}^{\bullet}$ consistently has the lowest formation energy of about 0.515−0.550 eV (details are shown in the Supporting Information). Our finding compares well with both existing theoretical and experimental studies of defects in $LiFePO_4$; using empirical potentials, Islam et al.[3,11] also determine that the formation energy for the bound antisite defect is the lowest of all considered defects ($E_{antisite}$ = 0.74 eV), and in studies by Chung et al.[12,13] using high-angle annular dark-field (HAADF) scanning transmission electron microscopy (STEM) antisite defects are observed with concentration ~1 % at 600 °C. At temperatures considered in this study, $Fe_{Li}^{\bullet}$ is expected to be comparatively immobile with respect to the time scale of Li^+ migration within the 1D channels, which is in line with the excellent cycling capability and capacity retention of this material.

Li^+ sites situated between $Fe_{Li}^{\bullet}$ defects cannot be reached from the surface of a particle unless there is an alternative transport path available (to be discussed later) and we refer to these Li^+ sites as part of the "blocked" capacity. While in very large particles most sites will be blocked by defects, the total channel length between surfaces in nanoparticles is small, resulting in channels containing very few or even zero defects. For instance, for particles smaller than 60 nm, 1 % $Fe_{Li}^{\bullet}$ population leads to on average fewer than two defects residing in each channel, and therefore no blocked Li^+ sites (the distance between Li^+ sites along the 1D channel in $LiFePO_4$ is ~3 Å). A more rigorous probabilistic model of the fraction of "unblocked" sites can be constructed assuming that the creation of defects is a Poisson process, the location of defects is spatially uniform, and the capacity situated between two defects in the same Li^+ ion channel (shown as red in Figure 1b) is blocked. The details of this derivation are described in the Supporting Information, but the mean fraction of unblocked capacity, C, (reachable from the surface without going through defects) is given by

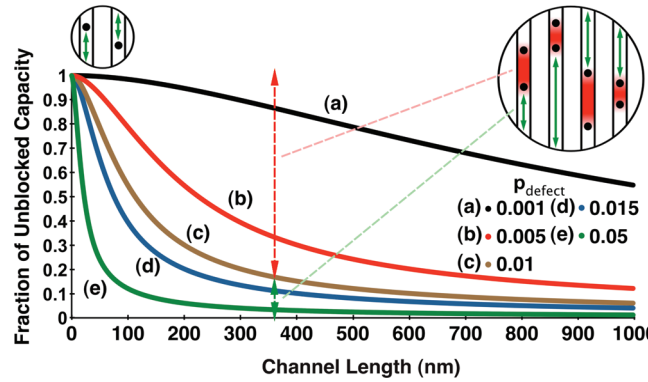

FIGURE 2. Expected unblocked capacity vs channel length in $LiFePO_4$ as determined by eq 1 for various defect concentrations.

$$C = \frac{2 - (2 + Np_{def})\exp(-Np_{def})}{-Np_{def}} \qquad (1)$$

where N is the number of Li^+ sites along a 1D channel, and p_{def} is the concentration of defects. The expected fraction of unblocked capacity (eq 1) as a function of one-dimensional channel length is plotted in Figure 2 for various defect concentrations. Given the formation energy of the bound antisite defect, the equilibrium defect concentration at typical solid-state synthesis temperatures (800−1100 K) is ~0.1−0.5 %, which can be considered as a theoretical thermodynamic limit representing a lower bound on the actual defect concentration in real materials, which are often synthesized via nonequilibrium techniques using precursors and contain trace quantities of impurities. Specifically, in $LiFePO_4$ single crystals grown by optical floating zone method, Amin et al.[14] observe ~2.5 − 3 % $Fe_{Li}^{\bullet}$, and in hydrothermally synthesized $LiFePO_4$ Yang et al.[15] observe up to ~7−8 % $Fe_{Li}^{\bullet}$.

The results in Figure 2 allow us to conceptualize how effective Li^+ mobility in $LiFePO_4$ may depend on particle size. For small particles, most of the channels will contain one or zero defects, and all sites are available by rapid diffusion through unblocked channels. For larger particles, most Li^+ sites will not directly be accessible from the surface. In the latter situation, the effective Li^+ diffusivity will be zero unless Li^+ ions can circumvent defects by migrating between different channels.

The Li_{Fe}^{-}−$Fe_{Li}^{\bullet}$ antisite defect offers such an opportunity for Li^+ to cross over between channels. To determine activation energies for Li^+ migration past $Fe_{Li}^{\bullet}$, we used the generalized gradient approximation (GGA) to density func-

DOI: 10.1021/nl1023595 | *Nano Lett.* **2010,** *10,* 4123–4127

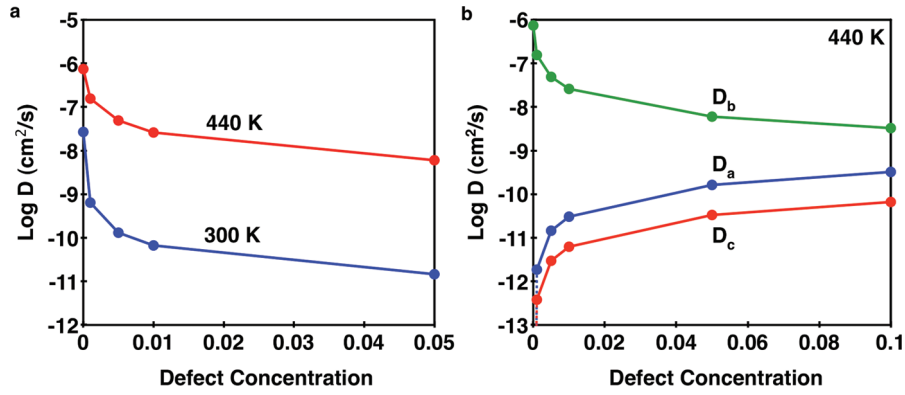

FIGURE 3. (a) Variation of the Li-vacancy self-diffusion along [010] with defect concentration at $T = 300$ K (red) and at $T = 440$ K (blue). (b) Variation of the Li-vacancy self-diffusion $D_{[100]}$ (blue), $D_{[010]}$ (green), and $D_{[001]}$ (red) with defect concentration at $T = 440$ K.

tional theory as implemented in the Vienna Ab Initio Simulation Package (VASP). Elastic band calculations were performed in supercells containing up to eight unit cells and four images in the dilute vacancy limit. Various migration paths conforming to Li^+ circumventing $Fe_{Li}^{\bullet}$ were considered, and it was determined that the lowest energy path possible occurs by Li^+ migrating to the nearest Li^+ channel through a vacant intermediate Fe^{2+} site with an activation barrier of 0.491 eV (details in Supporting Information).

Given the mechanism of defect circumvention and its migration barrier, we have determined the bulk diffusivity of lithium in $LiFePO_4$ containing defects by employing a modified random walk model (described in the Supporting Information) in a potential landscape with activation energies corresponding to fast 1D diffusion along the [010] direction and defect circumvention. Along the [010] direction, if the migrating atom does not neighbor a defect it is equally likely to move forward as backward in the Li^+ channel. However, if the migrating atom lies directly adjacent to the defect, it is likelier to move in the direction away from the defect rather than circumvent it because the activation barrier associated with a back-jump is much smaller, which leads to significantly reduced mean-square displacement and thus reduced diffusion coefficient with increasing defect concentration.

We discuss the vacancy diffusion over lithium sites as it is a more intrinsic property than the lithium diffusion that depends on the Li-vacancy concentration. The Li-vacancy concentration is set by the degree of lithiation (in the single-phase region) up to a maximum value reached at the solubility limit, estimated to be up to ~11% by Yamada et al.[16] The vacancy self-diffusion coefficient along [010] at 300 and 440 K as a function of defect concentration is shown in Figure 3a. To determine the Li^+ diffusivity in the dilute vacancy limit, the values shown in Figure 3 should be multiplied by a prefactor including the equilibrium vacancy concentration. The presence of defects is shown to significantly decrease the bulk 1D diffusivity along Li^+ tunnels even with defect concentrations less than 0.01. At room temperature, the drop in diffusivity is more drastic, reducing by more than 2 orders of magnitude with $p_{defect} = 0.005$ ($D_{[010]} = \sim 10^{-10}$ cm^2/s). It should be noted that the crossover mechanism involves a net displacement in the ⟨101⟩ directions and is consequently the predominant mechanism for diffusion in the [100] and [001] directions. At 440 K, $D_{[100]}$ and $D_{[001]}$ as a function of defect concentration are shown in Figure 3b and compare well with single-crystalline $LiFePO_4$ diffusivity measurements performed by Amin et al. who report ~2.5−3% antisite defects.[14,17] Compared to the defect-free scenario, there is a sharp reduction in the anisotropy of the diffusivity in the presence of defects that corroborates observations of 2D diffusion behavior.[14,17] The shift of a diffusion mechanism from 1D to either 2D or 3D due to the presence of defects is a general materials concept rather than a unique property of $LiFePO_4$, as the same phenomenological behavior has explained both the deviation from 1D diffusion of self-interstitial crowdion defects in materials undergoing irradiation damage[18] as well as the relative anisotropy of Li^+ conductivity in ramsdellite $Li_2Ti_3O_7$.[19]

To illustrate the effect of point defect obstructions on rate performance of $LiFePO_4$ across varying particle size and defect concentration, we look to the characteristic time (defined by (eq 2) and plotted in Figure 4) for Li^+ to diffuse along the [010] direction, which takes into account fast diffusion through unblocked capacity (governed by $D_{unblocked}$ as calculated by Morgan et al.[4]) and slower diffusion (governed by $D_{blocked}$ as shown in Figure 3a) through trapped capacity between defects

$$t = t_{blocked} + t_{unblocked} = \frac{x_{blocked}^2}{D_{blocked}} + \frac{x_{unblocked}^2}{D_{unblocked}} \quad (2)$$

The average blocked and unblocked diffusion lengths, $x_{blocked}$ and $x_{unblocked}$, are determined from the product of particle length and the fraction of blocked/unblocked capacity as calculated in eq 1. From Figure 4, the impact of defects is striking; even when the particle size is reduced to 100 nm,

DOI: 10.1021/nl1023595 | *Nano Lett.* **2010,** *10,* 4123–4127

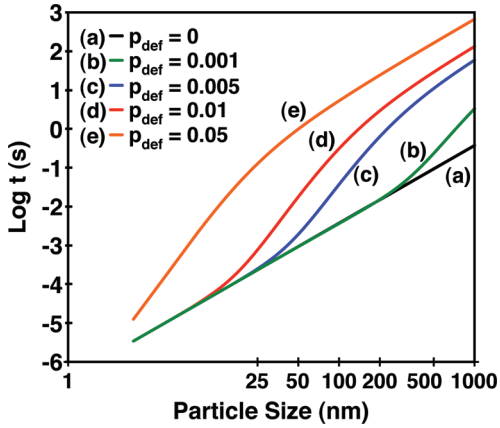

FIGURE 4. Characteristic diffusion time to traverse a particle along the [010] direction as defined by eq 2 plotted as a function of particle size for varying defect concentrations.

there is an order of magnitude decrease in the characteristic diffusion time with just 0.05% defect concentration and an additional order of magnitude decrease at 1% defect concentration.

In a $\log(t) - \log(x)$ plot, Fickian diffusion appears as a straight line with slope of two as diffusion time scales as the square root of distance. Figure 4 shows that this is only the case for a defect-free crystal. In the presence of point defects, power law behavior of time is only observed for very small particles (with high D) or very large particles (with smaller D). Hence, there is a particle size regime where diffusion transitions from the nanoregime to the bulk and diffusion times do not scale with length as one would expect from Fick's law.

In this work, we have demonstrated that the diffusion constant of ions moving in one-dimensional channels is not intrinsic, but determined by particle size as soon as point defects are present. These point defects restrict the root-mean square displacement of the ions and without migration paths around defects, the diffusion constant in a macroscopic crystal would tend to zero. Specifically for $LiFePO_4$, we confirmed with first principles methods that the channel-blocking defects are likely $Li_{Fe}^{\prime}$—$Fe_{Li}^{\bullet}$ antisites and that migration of Li^+ through the vacant Fe^{2+}-site is a much higher energy process than Li^+ migration within the channels. This process makes the diffusion constant of Li^+ dependent on both particle size and defect concentration. For small particles, most channels have zero or one defect in them, making all sites accessible by very rapid migration of Li^+ through the channels. For larger particles, multiple crossovers are required between channels to reach all Li^+ sites, making transport intrinsically slower. By calculating effective diffusion constants, we find that the impact of just modest concentrations of antisite defects is considerable; with >0.005 defect concentration, the fraction of unblocked capacity is negligible at the micrometer-scale, and the bulk diffusivity along the [010] direction decreases by over 2 orders of magnitude at room temperature. Also, by forcing crossover between Li^+ tunnels in large crystals, the dimensionality of the diffusion mechanism shifts from 1D to 2D or 3D as the anisotropy of the diffusion coefficients reduces in the presence of defects. Both of these findings reconcile discrepancies in the measurement of Li^+ diffusivity in $LiFePO_4$ across different particle sizes and synthesis methods. Specifically, the results of Amin et al.,[14,17] which show reduced Li^+ diffusivity and imply a 2D diffusion mechanism in millimeter-size $LiFePO_4$ single crystals, are well understood in the context of our model of Li^+ diffusion in the presence of defects. Without invoking surface effects and changes in solubility with particle size, the deleterious effect of channel-blocking point defects also provides a convincing argument as to why the general performance of nano-$LiFePO_4$ is so much better than its bulk counterpart.

In this study, we have focused on the impact of antisite defects, but we anticipate that off-stoichiometric defects involving $Fe_{Li}^{\bullet}$, albeit fewer in population due to higher formation energy, will have much higher Li^+ migration barriers for defect circumvention. For instance, the crossover migration of Li^+ past antisite defects as described earlier cannot occur in Fe-excess $LiFePO_4$ as all intermediate Fe^{2+} sites always remain occupied by Fe^{2+}. Consequently, any trapped capacity between two such defects may remain entirely inaccessible at any reasonable rate of charge/discharge.

While $LiFePO_4$ performs very well as a Li-battery cathode when in nanoform, the use of nanoparticles leads to lower packing density in the electrodes, reducing the energy density of batteries. For many applications, including portable electronics and electrified vehicles, the volume of the battery is as important a consideration as weight, and larger particle size $LiFePO_4$ could significantly increase the energy content of cells. Our results clarify that mitigation of channel-blocking point defects now becomes a critical design consideration in the $LiFePO_4$ synthesis process, and the remaining future challenge is to synthesize near defect-free $LiFePO_4$ at larger particle sizes. While we have explored the particle size effects that arise due to one-dimensional diffusion in defective $LiFePO_4$, the same concepts can be applied to other potential battery materials.

Acknowledgment. D.B. and M.B. were supported in part by the FRG Program of the National Science Foundation under Award numbers DMS-0855011 and DMS-0842504, and R.M. and G.C. were supported in part under Award number DMS-0853488. The defect work was supported by the Assistant Secretary for Energy Efficiency and Renewable Energy, Office of Vehicle Technologies of the U.S. Department of Energy under Contract No. DE-AC02-05CH11231, under the Batteries for Advanced Transportation Technologies (BATT) Program Subcontract no. 6806960. The diffusion work is based upon work supported as part of the Northeastern Center for Chemical Energy Storage, an Energy Frontier Research Center funded by the U.S. Department of

DOI: 10.1021/nl1023595 | *Nano Lett.* **2010,** *10,* 4123–4127

Energy, Office of Science, Office of Basic Energy Sciences under Award Number DE-SC0001294.

Supporting Information Available. Defect formation energies, derivation of unblocked capacity in $LiFePO_4$ channels containing defects, crossover migration path, and 1D random walk model. This material is available free of charge via the Internet at http://pubs.acs.org.

REFERENCES AND NOTES

(1) Delacourt, C.; Poizot, P.; Levasseur, S.; Masquelier, C. *Electrochem. Solid-State Lett.* **2006**, *9* (7), A352–A355.
(2) Padhi, A. K.; Nanjundaswamy, K. S.; Goodenough, J. B. *J. Electrochem. Soc.* **1997**, *144* (4), 1188–1194.
(3) Islam, M. S.; Driscoll, D. J.; Fisher, C. A. J.; Slater, P. R. *Chem. Mater.* **2005**, *17* (20), 5085–5092.
(4) Morgan, D.; Van der Ven, A.; Ceder, G. *Electrochem. Solid-State Lett.* **2004**, *7* (2), A30–A32.
(5) Nishimura, S.; Kobayashi, G.; Ohoyama, K.; Kanno, R.; Yashima, M.; Yamada, A. *Nat. Mater.* **2008**, *7* (9), 707–711.
(6) Huang, H.; Yin, S. C.; Nazar, L. F. *Electrochem. Solid-State Lett.* **2001**, *4* (10), A170–A172.
(7) Kang, B.; Ceder, G. *Nature* **2009**, *458* (7235), 190–193.
(8) Yamada, A.; Yonemura, M.; Takei, Y.; Sonoyama, N.; Kanno, R. *Electrochem. Solid-State Lett.* **2005**, *8* (1), A55–A58.
(9) Chen, D. P.; Maljuk, A.; Lin, C. T. *J. Cryst. Growth* **2005**, *284* (1−2), 86–90.
(10) Zhou, F.; Cococcioni, M.; Kang, K.; Ceder, G. *Electrochem. Commun.* **2004**, *6* (11), 1144–1148.
(11) Fisher, C. A. J.; Prieto, V. M. H.; Islam, M. S. *Chem. Mater.* **2008**, *20* (18), 5907–5915.
(12) Chung, S. Y.; Choi, S. Y.; Yamamoto, T.; Ikuhara, Y. *Phys. Rev. Lett.* **2008**, *100* (12), .
(13) Chung, S. Y.; Choi, S. Y.; Yamamoto, T.; Ikuhara, Y. *Angew. Chem., Int. Ed.* **2009**, *48* (3), 543–546.
(14) Amin, R.; Balaya, P.; Maier, J. *Electrochem. Solid-State Lett.* **2007**, *10* (1), A13–A16.
(15) Yang, S. F.; Song, Y. N.; Zavalij, P. Y.; Whittingham, M. S. *Electrochem. Commun.* **2002**, *4* (3), 239–244.
(16) Yamada, A.; Koizumi, H.; Nishimura, S. I.; Sonoyama, N.; Kanno, R.; Yonemura, M.; Nakamura, T.; Kobayashi, Y. *Nat. Mater.* **2006**, *5* (5), 357–360.
(17) Amin, R.; Maier, J.; Balaya, P.; Chen, D. P.; Lin, C. T. *Solid State Ionics* **2008**, *179* (27−32), 1683–1687.
(18) Heinisch, H. L.; Trinkaus, H.; Singh, B. N. *J. Nucl. Mater.* **2007**, *367*, 332–337.
(19) Boyce, J. B.; Mikkelsen, J. C. *Solid State Commun.* **1979**, *31* (10), 741–745.

DOI: 10.1021/nl1023595 | *Nano Lett.* **2010,** *10,* 4123–-4127